Int. J. Heat Mass Transfer. Vol. 35, No. 11, pp. 3085–3093, 1992
Printed in Great Britain

0017–9310/92 $5.00 + 0.00
Pergamon Press Ltd

Analytical and experimental investigation of the rewetting of circular channels with internal V-grooves

G. P. PETERSON† and X. J. LU
Department of Mechanical Engineering, Texas A&M University, College Station, TX 77843-3123, U.S.A.

and

X. F. PENG and B. X. WANG
Thermal Engineering Department, Tsinghua University, Beijing 100084, China

(*Received* 21 *October* 1991)

Abstract—Analytical and experimental investigations were conducted to determine the rewetting characteristics of capillary induced liquid flow in a circular channel with small circumferential grooves machined on the inner surface. Expressions for the rewetting velocity and maximum heat flux under which rewetting would occur were derived as functions of the thermal properties of liquid and channel, diameter of the circular channel and capillary radius of the circumferential wall grooves, and the input heat flux magnitude and distribution. Measurements of the radial position of the rewetting front and the maximum heat flux under which rewetting would occur were made for surfaces with different circumferential grooves and three different fluids, acetone, methanol and R11. The analytical expressions are in good agreement with the experimental data. The rewetting ability of these grooved surfaces was shown to decrease as the groove radius decreased, while the capillary pumping increases linearly with the groove radius.

INTRODUCTION

SEVERAL heat pipe configurations have been or currently are under consideration for use as radiator elements in low earth orbit, manned space platforms. Two of these, the Grumman monogroove heat pipe [1] and the Lockheed graded-groove heat pipe [2], shown in Figs. 1(a) and (b), are comprised of two parallel circular channels, one for vapor flow and one for liquid flow. The liquid and vapor channels in these heat pipes are connected by a small longitudinal slot to provide axial pumping while the small circumferential grooves on the inside of the vapor channel distribute the working fluid over the inner surface. Under normal operating conditions, heat supplied to the horizontal fin of the evaporator is conducted around the circumference of the vapor channel and through the heat pipe walls to these circumferential grooves where the working fluid is vaporized. Because of the high pressure associated with the increased temperature, the vapor in this region moves towards the cooler region where it condenses and gives up the latent heat of vaporization. The liquid is then 'pumped' back to the evaporator by the capillary forces in the longitudinal slot.

Under high thermal loads or adverse gravitational conditions, the longitudinal slot may not be capable of providing sufficient liquid to the circumferential wall grooves, resulting in dryout. When this occurs, it will be necessary to reduce the evaporator heat flux to allow the circumferential wall grooves to rewet. This rewetting process which results from the high capillary pressure induced by the small characteristic

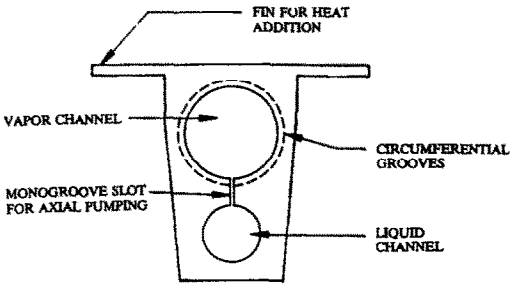

FIG. 1(a). Monogroove heat pipe [1].

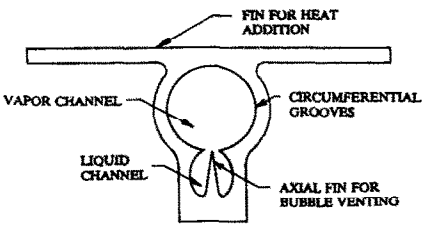

FIG. 1(b). Graded-groove heat pipe [2].

† To whom correspondence should be addressed.

NOMENCLATURE

c	specific heat of the channel
c'	experimental constant
F_{surf}	surface tension force
F_g	gravitational force
F_{fric}	wall friction force
g	gravitational acceleration
h	liquid rise height
h_f	latent heat of vaporization
k	thermal conductivity of the plate
Pr	Prandtl number
Q	total heat transferred
q''	heat flux
R	vapor channel radius
Re	Reynolds number
r	circumferential groove capillary radius
T	temperature
T_s	liquid saturation temperature
T_w	surface temperature at the rewetting front
t	time
U	average velocity of the liquid
U_w	rewetting velocity
u	local liquid velocity
w	groove width.

Greek symbols

α	thermal diffusivity
β	contact angle
γ	cone angle of groove
δ	thickness of the channel wall
θ	angle
θ'	angle in moving coordinate frame
θ_w	local angle of the rewetting front
μ	absolute viscosity
σ	surface tension.

Subscripts

l	liquid
max	maximum
w	wetting.

radius of the wall grooves is quite complex. Several researchers, including Elliott and Rose [3], Simopoules *et al.* [4], Stroes *et al.* [5], Ueda *et al.* [6, 7], Elias and Yadigaroglu [8] and Raj and Pate [9], have investigated the rewetting characteristics of liquid films on heated or hot rods, tubes, or flat surfaces. Saeed and Peterson [10] have reviewed the work of these and others and found that although these investigations have provided substantial experimental data and considerable insight into the behavior of thin films on both circular tubes and flat plates, no general physical model exists which is capable of describing the governing phenomena or the behavior of the liquid at or near the rewetting front.

Recently, Peng and Peterson [11–14] have proposed several models to predict the rewetting behavior for specific geometries. These include the wetting and rewetting of heated and unheated flat surfaces, and the rewetting of heated flat plates with a thin porous cover layer. In these models, the vaporization of the liquid at the rewetting front was assumed to be an important aspect of rewetting. Consequently, the rewetting velocity was first related to the liquid flow velocity and then exact analytical solutions were obtained to determine the rewetting velocity for a thin liquid film as a function of the bulk liquid flow velocity, the applied heat flux, and the thermophysical properties of the liquid and the surface over which the liquid was flowing. These theoretical analyses were then compared with several different sets of experimental data [15]. As a result of this work, a generalized model which describes the rewetting of flat heated plates was presented and discussed [16]. While this information is helpful, the rewetting process occurring on flat heated surfaces with a porous cover layer or a series of relatively large parallel grooves is significantly different from the case of a circular surface with circumferential grooves, of interest here.

ANALYSIS

In the evaporator section of the high capacity heat pipes, shown in Figs. 1(a) and (b), the grooves on the vapor channel wall are fabricated with a trapezoidal or V-shaped cross-section. The liquid flow in these grooves is driven by surface tension and, as a result, the liquid film will never be higher than the upper edge of the groove. This simplifies the problem considerably in that it allows each of the circumferential wall grooves to be evaluated independently. To further simplify the problem the solid surface is initially assumed to be at ambient conditions (i.e. not heated) and the liquid is assumed to wet the surface (i.e. the wetting angle is zero), forming a continuous film in each groove. For this case, the liquid film is subjected to a wall shear stress, a gravitational force, which may either assist or hinder the rewetting depending upon the orientation of the channel with respect to gravity, and a capillary driving force.

Unheated surfaces

If the entire liquid layer on the inner surface of the wall is taken as the control volume and the liquid mass is assumed to increase as the length of the liquid layer increases, the liquid layer length is fixed for a given time t and the liquid velocity is the same for any point in the control volume (by continuity). As a result the liquid film advances at an average tangential

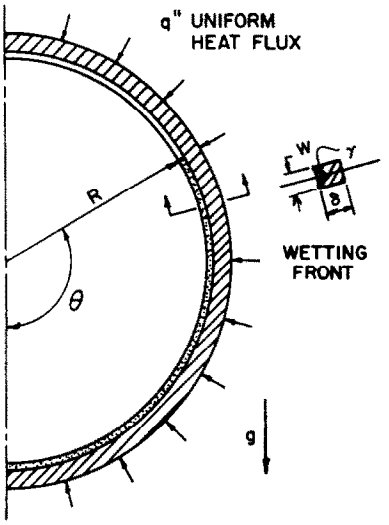

FIG. 2. Physical model.

velocity, U, which will vary with respect to the length of the liquid film. The physical model for this case is shown in Fig. 2. As illustrated, the flow is assumed to be one-dimensional curvilinear flow and the liquid film thickness is assumed to be constant along the groove, as are the thermophysical properties of both the liquid and the channel. In addition, the channel radius, R, is assumed to be very large compared with the groove width, w, and the thickness of channel wall, δ.

Based on the considerations above, Newton's law for the liquid film in the groove can be written as

$$F_{\text{surf}} - F_{\text{g}} - F_{\text{fric}} = \frac{\mathrm{d}}{\mathrm{d}t}(mU). \tag{1}$$

For a wetting fluid, the capillary driving force can be expressed as

$$F_{\text{surf}} = \frac{2\sigma}{r}\cdot\frac{w^2}{4}\operatorname{cotan}\frac{\gamma}{2} = \frac{\sigma w^2}{2r}\operatorname{cotan}\frac{\gamma}{2}. \tag{2}$$

The gravitational force is much more complex since the orientation of the groove with respect to the gravitational vector changes for different positions, but can be expressed as

$$\begin{aligned} F_{\text{g}} &= \int_0^{\theta} \frac{w^2}{4}\rho_{\text{l}} g \operatorname{cotan}\frac{\gamma}{2}\sin\theta R\,\mathrm{d}\theta \\ &= \tfrac{1}{4}w^2\rho_{\text{l}} g R \operatorname{cotan}\frac{\gamma}{2}\int_0^{\theta}\sin\theta\,\mathrm{d}\theta \\ &= \tfrac{1}{4}w^2\rho_{\text{l}} g R \operatorname{cotan}\frac{\gamma}{2}(1-\cos\theta). \end{aligned} \tag{3}$$

For Newtonian fluids in laminar flow, the shear stress at the wall is

$$C_{\text{w}} = \mu_{\text{l}}\left.\frac{\partial u}{\partial y}\right|_{\text{at wall}} \approx \mu_{\text{l}}\frac{U}{\frac{w}{5}} = \frac{5\mu_{\text{l}}U}{w}. \tag{4}$$

Using this value, an expression for the wall friction can be derived as

$$F_{\text{fric}} = 2w\theta R C_{\text{w}} = 2w\theta R\frac{5\mu_{\text{l}}U}{w} = 10\mu_{\text{l}}\theta R U \tag{5}$$

and because

$$m = \tfrac{1}{4}w^2 R\theta\rho_{\text{l}}\operatorname{cotan}\frac{\gamma}{2}, \tag{6}$$

$$\mathrm{d}(mU) = \tfrac{1}{4}w^2 R\rho_{\text{l}}\operatorname{cotan}\frac{\gamma}{2}\left(U\frac{\mathrm{d}\theta}{\mathrm{d}t} + \theta\frac{\mathrm{d}U}{\mathrm{d}t}\right). \tag{7}$$

The differential time, $\mathrm{d}t$, in equations (1) and (7) can be replaced by

$$\mathrm{d}t = \frac{R\,\mathrm{d}\theta}{U}. \tag{8}$$

Substituting equations (2), (3), (5), (7) and (8) into equation (1) yields

$$\begin{aligned} &\frac{\sigma w^2}{2r}\operatorname{cotan}\frac{\gamma}{2} - \tfrac{1}{4}\rho_{\text{l}} g w^2 R\operatorname{cotan}\frac{\gamma}{2}(1-\cos\theta) - 10\mu_{\text{l}}\theta R U \\ &\qquad = \tfrac{1}{4}w^2\rho_{\text{l}}\operatorname{cotan}\frac{\gamma}{2}\left(U^2 + \theta U\frac{\mathrm{d}U}{\mathrm{d}\theta}\right) \end{aligned} \tag{9}$$

or

$$\frac{\mathrm{d}U}{\mathrm{d}\theta} = \frac{\dfrac{\sigma w^2}{2r}\operatorname{cotan}\frac{\gamma}{2} - \tfrac{1}{4}\rho_{\text{l}} g w^2 R\operatorname{cotan}\frac{\gamma}{2}(1-\cos\theta) - 10\mu_{\text{l}}\theta R U - \tfrac{1}{4}w^2\rho_{\text{l}} U^2\operatorname{cotan}\frac{\gamma}{2}}{\tfrac{1}{4}w^2\rho_{\text{l}} U\theta\operatorname{cotan}\frac{\gamma}{2}} \tag{10}$$

with boundary conditions

$$\theta = 0, \quad U = 0. \tag{11}$$

Equation (10) represents an expression for the rewetting velocity, U, as a function of the angular position of the wetting front, θ, and assumes the surface is at ambient conditions with no heat addition. Because of the functional dependence of the velocity on position, a direct analytical solution is not possible and, hence, a numerical technique must be employed.

Heated surfaces

For the case of rewetting of a surface after dryout, the liquid front is assumed to be driven by capillary pressure and to advance along the grooves in the channel wall to which a uniform circumferential heat flux, q'', has been applied, as shown in Fig. 2. Because the surface is at an elevated temperature (at or near the Leidenfrost temperature), some of the liquid at the leading edge of the advancing liquid front is vaporized. The remaining liquid advances with a velocity U_{w}, referred to as the wetting front velocity. The heat required to vaporize this liquid is supplied by conduction from the dry hot zone of the channel surface. When dryout occurs the heat supplied to the wetting front exceeds that required to vaporize all of the

liquid. For the case of no heat addition previously described, no vaporization occurs and the wetting front velocity and liquid velocity are equal. However, for a heated plate the liquid velocity is higher than the wetting front velocity, since some of the liquid is vaporized, reducing the liquid mass flow rate.

To determine the amount of heat absorbed by the vaporization process, the conduction equation for the channel wall can be transformed to a coordinate system moving with a velocity equal to that of the wetting front, U_w. In this analysis, a curvilinear coordinate system was again employed and the conduction through the walls was assumed to be one-dimensional. Several other fundamental assumptions were made and can be summarized as follows:

1. The grooves on the surface were assumed to be located immediately adjacent to one another and the sizes of the grooves were assumed to be much smaller than the thickness of the wall (i.e. $w \ll \delta$).
2. The liquid temperature at the rewetting front was assumed to be different from the rewetting temperature, which was assumed to be constant and equal to the saturation temperature, T_s.
3. The convective heat transfer between the plate and the vapor, along with radiation from both the heated surface and the vapor, was neglected.

Utilizing these assumptions, the conduction equation for the wall can be written as:

$$\frac{k}{R^2}\frac{\partial^2 T}{\partial \theta'^2} + \frac{q}{\delta} = \rho c \frac{\partial T}{\partial t} \tag{12}$$

or

$$k\frac{d^2T}{d\theta'^2} + \frac{q''R^2}{\delta} = \rho c R U_w \frac{dT}{d\theta'}. \tag{13}$$

The general solution of equation (12) is

$$T = C_1 + C_2 \exp\left[\frac{\rho c U_w R\theta'}{k}\right] + \frac{q''R\theta'}{\rho c U_w \delta}. \tag{14}$$

If the circular grooves are assumed to have a finite length, the location and condition at the groove ends are difficult to determine, especially in a moving system. However, the problem of interest here is the prediction of the heat conduction at the wetting front, and it is therefore reasonable to develop a solution assuming infinite grooves. Differentiating equation (14) with respect to θ' yields

$$\frac{dT}{d\theta'} = C_2\left(\frac{lcU_wR}{k}\right)\exp\left[\frac{\rho c U_w R\theta'}{k}\right] + \frac{q''R}{\rho c U_w \delta}. \tag{15}$$

This expression indicates that equation (15) will approach infinity as $\theta' \to \infty$, which is not physically possible. Therefore, $C_2 = 0$ and at the rewetting front the plate temperature is at the Leidenfrost or rewetting temperature, i.e. $\theta' = 0$, $T = T_w$. Using this condition, a solution for equation (15) can be found as

$$T(\theta') = T_w + \frac{q''R}{\rho c U_w \delta}\theta'. \tag{16}$$

From this expression, the total heat conduction at $\theta' = 0$ can be found as

$$Q = \left(\delta w - \tfrac{1}{4}w^2 \operatorname{cotan}\frac{\delta}{2}\right)k\frac{dT}{Rd\theta'}\bigg|_{\theta'=0} \approx \frac{wq''\alpha}{U_w}. \tag{17}$$

Utilizing an energy balance, the total heat conduction in the region of the wetting front is equal to the energy absorbed by the liquid evaporation or

$$Q = \tfrac{1}{4}(U - U_w)\rho_l h_f w^2 \operatorname{cotan}\frac{\gamma}{2} \tag{18}$$

where U is determined from equation (10). As noted by Peng and Peterson [12], at the rewetting front liquid sputtering may be significant and some liquid may leave the groove as droplets due to the explosive forces resulting from boiling. Therefore in actuality, the amount of vaporized liquid predicted by equation (18) may be slightly higher than the amount actually vaporized at the wetting front. To compensate for this, an expression for the thermal boundary layer thickness for laminar flow presented by Kays and Crawford [17],

$$\frac{\delta_t}{x} = 4.64 Re_x^{-1/2} Pr_l^{-1/3}, \tag{19}$$

was modified as

$$\frac{\delta_t}{w} = c' Re_w^{-1/2} Pr_l^{-1/3} \tag{20}$$

where δ_t represents the thickness of liquid layer, c' is an experimentally determined constant, and the rewetting Reynolds number is defined as

$$Re_w = \frac{\rho_l U w}{\mu_l}. \tag{21}$$

Also, for a liquid layer of thickness δ_t, equation (18) becomes

$$Q = (U - U_w)\frac{w}{\sin\dfrac{\gamma}{2}}\delta_t \rho_l h_f \tag{22}$$

and combining equations (17) and (22) yields a quadratic expression of the form

$$\frac{(U - U_w)\delta_t \rho_l h_f}{\sin\dfrac{\gamma}{2}} = \frac{q''\alpha}{U_w}. \tag{23}$$

Substituting equation (20) into equation (23) and rearranging yields

$$U_w^2 - UU_w + \frac{q''\alpha \sin\dfrac{\gamma}{2}}{c'\rho_l h_f w Re_w^{-1/2} Pr_l^{-1/3}} = 0 \tag{24}$$

and solving this expression for the rewetting velocity yields

$$U_w = \frac{1}{2}\left[U \pm \left(U^2 - \frac{4q''\alpha \sin\frac{\gamma}{2}}{c'\rho_l h_f w Re_w^{-1/2} Pr_l^{-1/3}}\right)^{1/2}\right]. \quad (25)$$

Previous analyses by Peng and Peterson [12] indicated that this solution is correct only when the second term on the right hand side is positive. Hence, the rewetting velocity can be expressed as

$$U_w = \frac{1}{2}\left[U + \left(U^2 - \frac{4q''\alpha \sin\frac{\gamma}{2}}{c'\rho_l h_f w Re_w^{-1/2} Pr_l^{-1/3}}\right)^{1/2}\right]. \quad (26)$$

For rewetting to occur, the following expression must be true:

$$U^2 - \frac{4q''\alpha \sin\frac{\gamma}{2}}{c'\rho_l h_f w Re_w^{-1/2} Pr_l^{-1/3}} \geq 0 \quad (27)$$

where the limiting conditions are

$$q_{max} = \frac{c'(\rho_l \mu_l)^{1/2} w^{1/2} h_f}{4 Pr_l^{1/3} \alpha \sin\frac{\gamma}{2}} U^{3/2}. \quad (28)$$

This limiting condition indicates the maximum heat flux under which rewetting can occur. Since the liquid velocity corresponds to the angular position, the maximum heat flux is different for every angular location and the liquid wetting front will exhibit a maximum angular position or rise height for any specified heat flux, q''.

EXPERIMENTAL INVESTIGATION

As noted above, the rewetting of trapezoidal or triangular grooves machined into the inside of circular channels has not been previously investigated either experimentally or analytically. The analysis presented here provides some basis for a better understanding; however, additional experimental data are required to better understand the phenomena which govern the liquid and rewetting behavior in this particular physical system and to determine the empirical constant, c', appearing in equations (26) and (28).

Experimental test facility

The experimental facility employed in this investigation is illustrated schematically in Fig. 3, and includes the test section, the liquid pool and a power source. Three circular test sections, each 25.4 mm in diameter, were fabricated from a 0.765-mm-thick stainless steel plate. A series of V-shaped grooves with an apex angle of grooves, γ, of 60° was machined into the inner surface of each of the three plates. The widths of the three sets of grooves were 0.635, 0.381 and 0.17 and the resulting physical characteristics associated with each are summarized in Table 1.

Three different working fluids, R11, methanol and acetone, were used as the working fluid for the experimental investigation. The test section was directly connected to a large power transformer and heated by direct current supplied to the stainless steel plate. To accurately measure the liquid rise and angular position, each of the three circular test sections were marked with an incremental scale prior to bending. This resulted in a means by which the wetting front could be determined to within an experimental uncertainty of approximately ±1.0°. The heat flux applied to the circular plate was determined by measuring the voltage and current supplied and could be determined to within ±1.5% over the entire range tested.

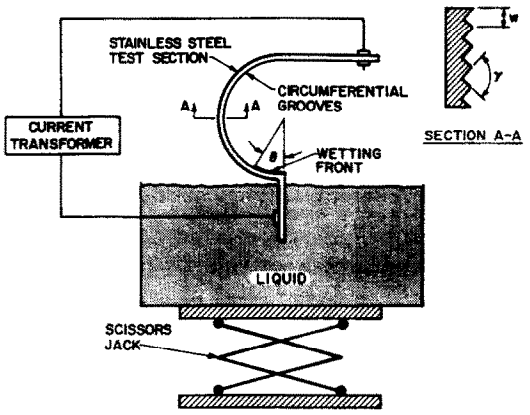

FIG. 3. Experimental test facility.

Experimental procedure

The experimental procedure utilized was to first heat the plates until the wall temperature was higher than the boiling temperature corresponding to the ambient pressure, approximately 80–160°C. The liquid pool was then raised until the liquid level reached a position level with the top of the grooves at an angular position of zero. After the liquid rise height had reached a maximum steady-state value, the location of the liquid front angle, along with the current and voltage, were measured and recorded. No attempt was made to measure the rewetting velocity in this experiment.

The principle driving force in equation (1) is the capillary pressure term, which depends on the liquid properties and the groove size. Because of the uncertainty of the wetting angle, the effective capillary radius for each of the three different grooves was

Table 1. Properties of grooves

No.	Width (mm)	Cone angle (degrees)	Capillary radius (mm)	Deviation of capillary radius (%)
1	0.635	60	0.26	1.0
2	0.381	60	0.19	1.2
3	0.177	60	0.14	1.2

determined experimentally using the following expression:

$$h = \frac{2\sigma}{\rho_l g r}. \tag{29}$$

The resulting average capillary radii for the three different sets of grooves are summarized in Table 1.

RESULTS AND DISCUSSION

The expression given in equation (10) with the boundary conditions shown in equation (11) was solved numerically for each of the three working fluids, and Figs. 4(a), (b) and (c) illustrate the results for all three working fluids and groove widths of 0.635, 0.381 and 0.177 mm, respectively. As illustrated, the liquid velocity as a function of the angular position is considerably different for the three fluids. In addition, comparison of these results for the three different sizes of grooves clearly indicates that the liquid velocity is strongly dependent upon the groove width.

Figures 5(a), (b) and (c) illustrate the relationship that exists between the uniformly applied heat flux and the maximum radial position (or rise height) for the three different groove widths. Each figure illustrates the experimental results for the three working fluids evaluated and compares these results with the values predicted by the analytical model, equation

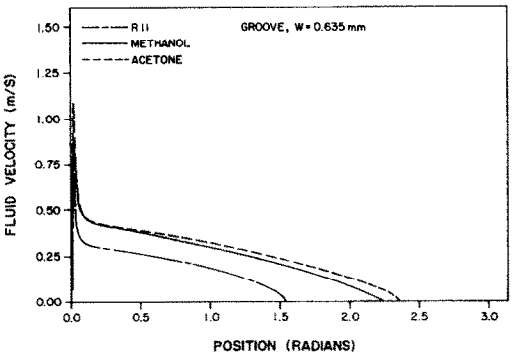

FIG. 4(a). Fluid velocity as a function of radial position for an unheated plate with 0.635-mm-wide grooves.

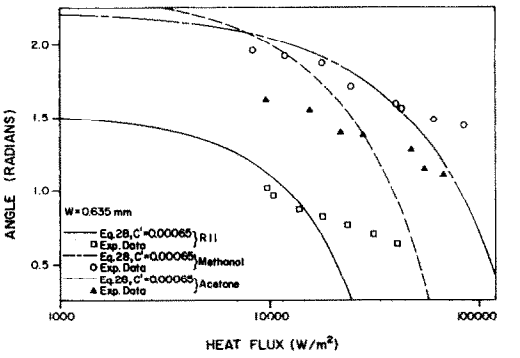

FIG. 5(a). Maximum rewetting angle as a function of input heat flux for a plate with 0.635-mm-wide grooves.

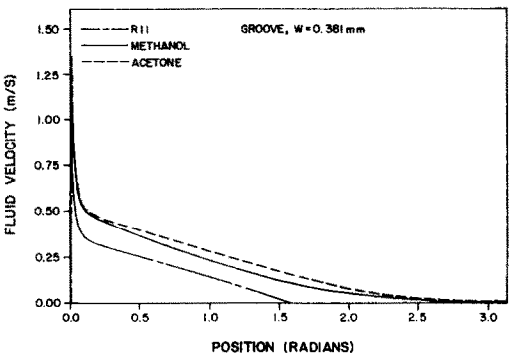

FIG. 4(b). Fluid velocity as a function of radial position for an unheated plate with 0.381-mm-wide grooves.

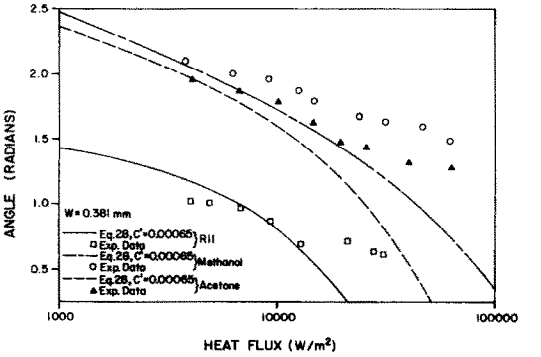

FIG. 5(b). Maximum rewetting angle as a function of input heat flux for a plate with 0.381-mm-wide grooves.

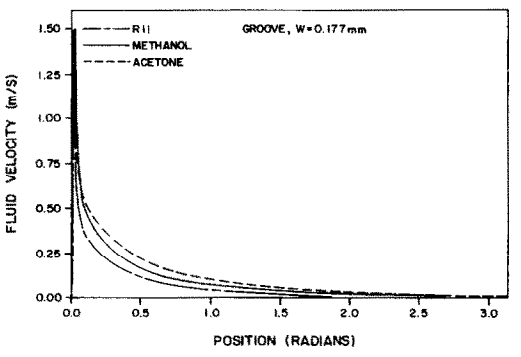

FIG. 4(c). Fluid velocity as a function of radial position for an unheated plate with 0.177-mm-wide grooves.

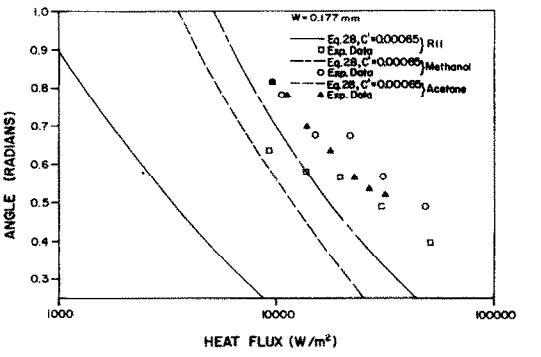

FIG. 5(c). Maximum rewetting angle as a function of input heat flux for a plate with 0.177-mm-wide grooves.

(28), using a value of $c' = 0.00065$. The rewetting experimental data for the surface with 0.635-mm-wide grooves indicate that the rewetting front position for methanol is largest and that for R11 is smallest (see Fig. 5(a)) for a given applied heat flux. Similar results (Fig. 5(b)) are shown for the surface with 0.381-mm-wide grooves. However, for the surface with 0.177-mm-wide grooves, the rewetting front angles for methanol and acetone approach each other at a given heat flux, and that of R11 is only slightly smaller. The results of the numerical model given in Figs. 4(a), (b) and (c) help to explain this phenomena. When no heat is applied to the surface of the test section with 0.177 mm grooves (Fig. 4(c)), the liquid velocity and mass flux are quite small and indicate only a very slight difference for the three liquids. In the experimental tests, the liquid flowing along the grooves is not sufficient to cool the surface and replenish the liquid vaporized and/or sputtered at the rewetting front. As a result, the liquid rise angle is much smaller and appears to be approximately the same for all three liquids.

To better illustrate the effect of groove size, the experimental data for methanol, acetone and R11 flowing in all three grooved surfaces are compared in Figs. 6(a), (b) and (c), respectively. The results indicate that there is no significant difference between the data for surfaces with 0.635-mm-wide grooves and those with 0.381-mm-wide grooves. However, the liquid rise for the surface with 0.177-mm-wide grooves is significantly lower than for the other two surfaces. The experimental results for R11 (Fig. 6(c)) indicate that the liquid front position essentially decreases as the groove width becomes smaller for a specified applied heat flux.

Based on the experimental data and the corresponding numerical results for liquid velocity given by equation (10), the coefficient c' in equation (28) was determined empirically and found to be 0.00065 for all cases investigated here. As mentioned previously, the theoretical results predicted by equation (28) with $c' = 0.00065$ are also shown in Figs. 5 and 6 for the three different liquids and three different grooved surfaces. As illustrated, these predicted values are in reasonably good agreement with the measured data. Also as illustrated, the empirical constant c' appears to be independent of the liquid properties and groove size and can therefore be assumed to be a universal constant for this and other rewetting processes.

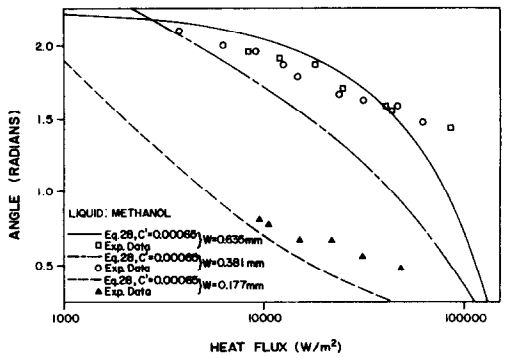

FIG. 6(a). Maximum rewetting angle as a function of input heat flux for methanol.

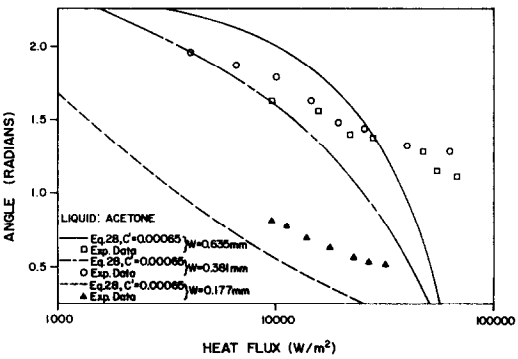

FIG. 6(b). Maximum rewetting angle as a function of input heat flux for acetone.

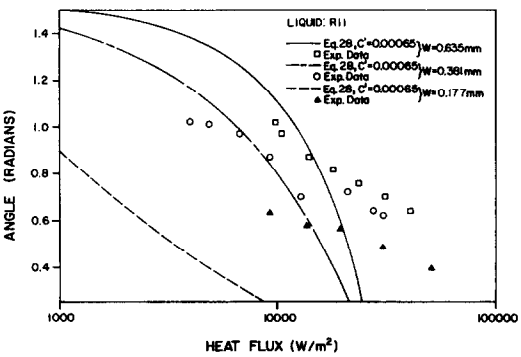

FIG. 6(c). Maximum rewetting angle as a function of input heat flux for R11.

CONCLUSIONS

A theoretical investigation has been conducted and a physical model developed to determine the rewetting characteristics of capillary induced liquid flow in a circular channel with microgrooves on the inside surface. This investigation provides a theoretical description of the mechanisms that govern the rewetting of these surfaces. The rewetting velocity was found to be a function of the thermal properties of the liquid and the channel, the input heat flux, the radius of the grooves and the circular channel, and the location of the liquid front. The maximum heat flux under which rewetting would occur was found to be a function of all these factors plus the input heat flux distribution.

An experimental investigation was conducted in parallel with the analytical study to verify the modeling technique and determine the maximum rewetting position as a function of the applied heat flux. Comparison of the analytical and experimental results indicated good agreement and demonstrated that the rewetting front position as a function of the applied heat flux could be determined for the two proposed

heat pipe configurations with a reasonably high degree of accuracy.

For most practical heat pipe applications, including those shown in Fig. 1, the circumferential wall grooves utilized are very small in order to result in a high 'pumping' capacity. This relationship between groove radius and pumping capacity is evident in Figs. 4(a), (b) and (c) and is well understood. However, for the rewetting of hot surfaces after dryout, the theoretical and experimental results illustrated in Figs. 5 and 6 indicate that because the rewetting area of small grooves is less than that of larger grooves, the amount of liquid supplied to the wall grooves is not sufficient to cool the surface and replenish the amount vaporized and sputtered at the rewetting front. This observation indicates that while the pumping capacity of the wall grooves in these types of heat pipes is directly related to the radius, the rewetting capacity decreases as the width of the groove radius decreases.

REFERENCES

1. J. Alario, R. Haslett and R. Kossan, The monogroove high performance heat pipe, AIAA Paper No. AIAA-81-1156, *16th AIAA Thermophysics Conf.*, Palo Alto, CA (June 1981).
2. J. H. Ambrose and H. R. Holmes, Development of the single graded groove high-performance heat pipe, AIAA-91-0366, AIAA Aerospace Sciences Meeting, Reno, NV (January 1991).
3. D. F. Elliott and P. W. Rose, The quench of a heated surface by a film of water in a steam environment at pressure up to 53 bar, Report No. AEIW-M976, Atomic Energy Establishment, Winfrith, U.K. (1970).
4. S. E. Simopoules, A. A. El-Shiribini and W. Murgatroyd, Experimental investigation of the rewetting process in a Freon-113 vapor environment, *Nucl. Engng Des.* **55**, 17–24 (1979).
5. G. Stroes, D. Fricker, F. Issacci and I. Catton, Heat flux induced dryout and rewet in thin films, *Proc. Ninth Int. Heat Transfer Conf.*, Vol. 6, pp. 358–364 (1990).
6. T. Ueda, M. Inoue, Y. Iwata and Y. Sogawa, Rewetting of a hot surface by a falling liquid film, *Int. J. Heat Mass Transfer* **26**, 401–410 (1983).
7. T. Ueda, S. Tsunenori and M. Koyanagi, An investigation of critical heat flux and surface rewet in flow boiling systems, *Int. J. Heat Mass Transfer* **26**, 1189 (1983).
8. E. Elias and G. Yadigaroglu, A general one-dimensional model for conduction-controlled rewetting of a surface, *Nucl. Engng Des.* **42**, 185–186 (1977).
9. V. V. Raj and A. W. Pate, Analysis of conduction controlled rewetting of hot surfaces based on two-region model, Paper No. IP-20, *Proc. Eighth Int. Heat Transfer Conf.*, Vol. 4, pp. 1987–1992 (1986).
10. B. Saced and G. P. Peterson, A review of rewetting of hot surfaces, *32nd Heat Transfer and Fluid Mechanics Inst.*, Vol. 32, pp. 203–237 (June 1991).
11. X. F. Peng and G. P. Peterson, Analytical investigation of the rewetting characteristics of heated plates with grooved surfaces, *AIAA J. Thermophys. Heat Transfer* (in press).
12. X. F. Peng and G. P. Peterson, Rewetting analysis for surface tension induced flow. In *Phase Change Heat Transfer*, Vol. HTD-159, pp. 69–75. ASME, New York (1991).
13. X. F. Peng, G. P. Peterson and B. X. Wang, Capillary induced rewetting in a flat porous cover layer, *Int. J. Heat Mass Transfer* **35**, 319–327 (1992).
14. X. F. Peng and G. P. Peterson, Experimental investigation of capillary investigation of capillary induced rewetting in a flat porous cover layer, *Annual Meeting, Proc. 1991 ASME Winter*, Atlanta, GA (1–6 December 1991).
15. X. F. Peng, G. P. Peterson and B. X. Wang, The effect of plate temperature on the onset of wetting, *Int. J. Heat Mass Transfer* **35**, 1605–1613 (1992).
16. X. F. Peng, G. P. Peterson and B. X. Wang, On the wetting mechanism of liquid flow on hot surfaces, *Int. J. Heat Mass Transfer* **35**, 1615–1624 (1992).
17. W. M. Kays and M. E. Crawford, *Convective Heat and Mass Transfer*. McGraw-Hill, New York (1990).

ETUDE ANALYTIQUE ET EXPERIMENTALE DU REMOUILLAGE DES CANAUX CIRCULAIRES AVEC DES RAINURES INTERNES EN V

Résumé—On conduit une étude analytique et expérimentale pour déterminer les caractères du remouillage par l'écoulement liquide induit par la capillarité, dans un canal circulaire avec des petites rainures circonférentielles usinées sur la surface interne. Des expressions pour la vitesse de remouillage et pour le flux thermique maximal au remouillage sont obtenues en fonction des propriétés thermiques du liquide et du canal, du diamètre du canal, du rayon capillaire des rainures, de la grandeur et de la distribution du flux thermique à l'entrée. Des mesures sur la position radiale du front de remouillage et sur le flux thermique maximal au remouillage sont faites pour différentes rainures circonférentielles et trois fluides différents : acétone, méthanol et R11. Les expressions analytiques sont en bon accord avec les données expérimentales. L'aptitude au remouillage diminue quand le rayon de la rainure décroît, alors que le pompage capillaire augmente linéairement avec le rayon de la rainure.

ANALYTISCHE UND EXPERIMENTELLE UNTERSUCHUNG DER WIEDERBENETZUNG KREISFÖRMIGER KANÄLE MIT INTERNEN V-FÖRMIGEN RILLEN

Zusammenfassung—Zur Untersuchung der durch Kapillarkräfte verursachten Wiederbenetzung von kreisförmigen Kanälen mit kleinen, in Umfangsrichtung über der Innenseite verteilten Rillen werden analytische und experimentelle Betrachtungen durchgeführt. Hierbei werden Ausdrücke für die Benetzungsgeschwindigkeit und die maximale Wärmestromdichte, unter welcher noch eine Benetzung auftritt, entwickelt. Die Ausdrücke sind Funktionen der thermischen Eigenschaften von benetzender Flüssigkeit und Kanal, sowie des Durchmesses der kreisrunden Kanäle, des Kapillaradius der Rillen und der Intensität und Verteilung der Wärmestromdichte. Messungen der radialen Position der Benetzungsfront und der maximalen Wärmestromdichte, unter der noch Benetzung eintritt, werden für Oberflächen mit unterschiedlichen Rillen und den drei Fluiden (Aceton, Methanol und R 11) durchgeführt. Die analytischen Lösungen stimmen gut mit den experimentellen Ergebnissen überein. Es wird gezeigt, daß die Fähigkeit zur Wiederbenetzung der Oberflächen mit dem Rillenradius abnimmt, während die geförderte Menge linear mit dem Rillenradius steigt.

АНАЛИТИЧЕСКОЕ И ЭКСПЕРИМЕНТАЛЬНОЕ ИССЛЕДОВАНИЯ ПОВТОРНОГО СМАЧИВАНИЯ КРУГОВЫХ КАНАЛОВ С ВНУТРЕННИМИ V—ОБРАЗНЫМИ КАНАВКАМИ

Аннотация—Аналитически и экспериментально исследовались характеристики течения жидкости за счет капиллярныхх сил в круговом канале с небольшими канавками, расположенными по окружности на внутренней поверхности. Получены выражения для скорости повторного смачивания и максимального теплового потока, при котором может произойти повторное смачивание, как функций тепловых характеристик жидкости и канала, диаметра кругового канала и капиллярного радиуса канавок, а также величины и распределения подводимого теплового потока. Для поверхностей с канавками различных размеров и трех различных жидкостей (ацетон, метанол и R11) проведены измерения радиального расположения фронта повторного смачивания и максимального теплового потока, при котором оно может произойти. Результаты расчетов по аналитическии выражениям хорошо согласуются с экспериментальными данными. Показано, что способность поверхностей с канавками к повторному смачиванию снижается с уменьшением радиуса канавок, а капиллярная прокачка линейно возрастает с его увеличением.